Inorg. Chem. **2003**, *42*, 2577−2583

The Effect of Ligand Scaffold Size on the Stability of Tripodal Hydroxypyridonate Gadolinium Complexes

Brendon O'Sullivan,[†] Dan M. J. Doble,[†] Marlon K. Thompson,[†] Carsten Siering,[†] Jide Xu,[†] Mauro Botta,[‡] Silvio Aime,[§] and Kenneth N. Raymond*,[†]

Department of Chemistry, University of California, Berkeley, California 94720, Dipartimento di Scienze e Tecnologie Avanzate, Università del Piemonte Orientale "Amedeo Avogadro", Corso Borsalino 54, I-15100 Alessandria, Italy, and Dipartimento di Chimica I.F.M., Università di Torino, Via P. Giuria 7, I-10125 Torino, Italy

Received November 6, 2002

The variation of the size of the capping scaffold which connects the hydroxypyridonate (HOPO) binding units in a series of tripodal chelators for gadolinium (Gd) complexes has been investigated. A new analogue of TREN-1-Me-3,2-HOPO (**1**) (TREN = tri(ethylamine)amine) was synthesized: TREN-Gly-1-Me-3,2-HOPO (**2**) features a glycine spacer between the TREN cap and HOPO binding unit. TRPN-1-Me-3,2-HOPO (**3**) has a propylene-bridged cap, as compared to the ethylene bridges within the TREN cap of the parent complex. Thermodynamic equilibrium constants for the acid–base properties of **2** and the Gd^{3+} complexation strength of **2** and **3** were measured and are compared with that of the parent ligand. The most basic ligand is **2** while **3** is the most acidic. Both **2** and **3** form Gd^{3+} complexes of similar stability (pGd = 16.7 and 15.6, respectively) and are less stable than the parent complex Gd-**1** (pGd = 19.2). Two of the three complexes are more stable than the bis(methylamide)diethylenetriamine pentaacetate complex Gd(DTPA-BMA) (pGd = 15.7) while the other is of comparable stability. Enlargement of the ligand scaffold decreases the stability of the Gd^{3+} complexes and indicates that the TREN scaffold is superior to the TRPN and TREN-Gly scaffolds. The proton relaxivity of Gd-**2** is 6.6 mM^{-1} s^{-1} (20 MHz, 25 °C, pH 7.3), somewhat lower than the parent Gd-**1** but higher than that of the MRI contrast agents in clinical practice. The pH-independent relaxivity of Gd-**2** is uncharacteristic of this family of complexes and is discussed.

Introduction

The effectiveness of magnetic resonance imaging (MRI) as a diagnostic tool is enhanced by the administration of gadolinium(Gd)-based contrast agents.[1−3] The clinically approved MRI contrast agents are based on an octadentate poly(aminocarboxylate) ligand scaffold and feature a nine-coordinate Gd^{3+} with a single coordinated water molecule. They are mostly structural derivatives of DTPA and DOTA and are thermodynamically stable, which is important due to the toxicity of free Gd^{3+}.[4] The development of second-generation contrast agents which target specific tissues and organs requires increased scrutiny of the thermodynamic stability of Gd^{3+} complexes as the in vivo residence time is lengthened.

Hexadentate tripodal hydroxypyridonate ligands of the TREN-1-Me-3,2-HOPO (**1**) type (Figure 1) form stable, diaquo complexes with Gd^{3+}.[5−7] [Gd(TREN-1-Me-3,2-HOPO)$(H_2O)_2$] (Gd-**1**) is the parent member of this series of complexes and possesses several characteristics which are desirable in an MRI contrast agent.[5] The relaxivity (r_1) of Gd-**1** is 10.5 mM^{-1} s^{-1} (37 °C, 20 MHz), some 2.5 times

* To whom correspondence should be addressed. E-mail: raymond@socrates.berkeley.edu.
[†] University of California.
[‡] Università del Piemonte Orientale "Amedeo Avogadro".
[§] Università di Torino.

(1) Aime, S.; Botta, M.; Fasano, M.; Terreno, E. *Chem. Soc. Rev.* **1998**, *27*, 19−29.
(2) Aime, S.; Fasano, M.; Terreno, E.; Botta, M. In *The Chemistry of Contrast Agents in Medical Magnetic Resonance Imaging*; Merbach, A. E., Toth, E., Eds.; Wiley: New York, 2001.
(3) Caravan, P.; Ellison, J. J.; McMurry, T. J.; Lauffer, R. B. *Chem. Rev.* **1999**, *99*, 2293−2352.
(4) Cacheris, W. P.; Quay, S. C.; Rocklage, S. M. *Magn. Reson. Imaging* **1990**, *8*, 467−481.
(5) Xu, J.; Franklin, S. J.; Whisenhunt, D. W.; Raymond, K. N. *J. Am. Chem. Soc.* **1995**, *117*, 7245−7246.
(6) Johnson, A. R.; O'Sullivan, B.; Raymond, K. N. *Inorg. Chem.* **2000**, *39*, 2652−2660.
(7) Hajela, S.; Botta, M.; Giraudo, S.; Xu, J.; Raymond, K. N.; Aime, S. *J. Am. Chem. Soc.* **2000**, *122*, 11228−11229.

10.1021/ic0261575 CCC: $25.00
Published on Web 03/18/2003

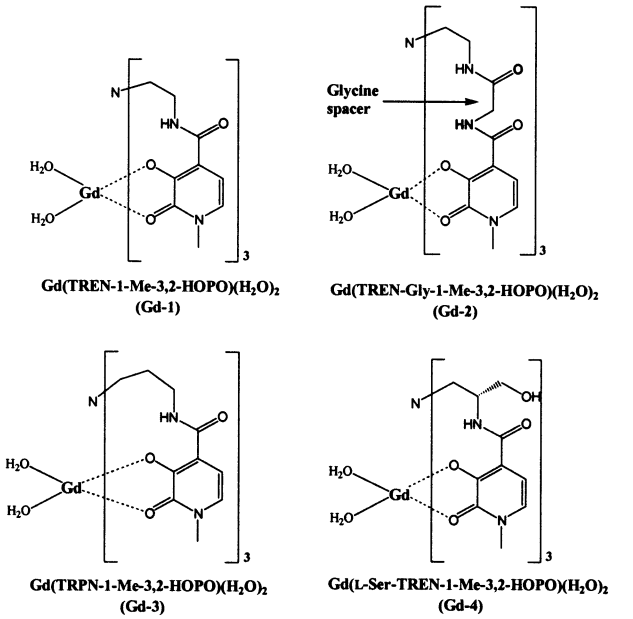

Figure 1. Tripodal Gd^{3+} hydroxypyridonate complexes described in this paper.

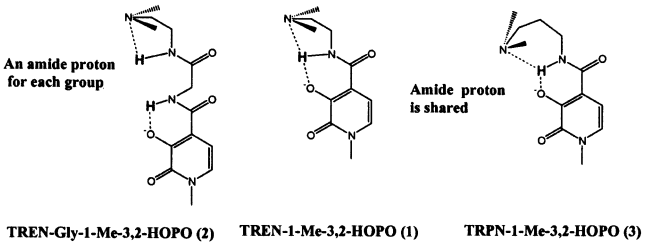

Figure 2. Intramolecular hydrogen bonding in the complexes discussed.

that of the widely used diethylenetriaminepentacetate complex $[Gd(DTPA)(H_2O)]^{2-}$. This is due to the higher number of metal-coordinated water molecules (q), fast inner-sphere water exchange, and the increased molecular weight (which results in a longer rotational correlation time, τ_r).[7]

Compound **1** exhibits (in comparison with DTPA, the bis(methylamide) DTPA-BMA, and the macrocyclic tetraaminetetraacetate DOTA) enhanced affinity and selectivity for Gd^{3+} over the physiological metal ions Ca^{2+} and Zn^{2+}, which indicates that the dissociation of Gd-**1** would be minimal in vivo. The low toxicity of **1** to mice has been demonstrated in preclinical trials.[8] The high stability of Gd-**1** is attributed to the internal hydrogen bonding between the amide proton and (i) the proximal phenolic oxygen of the hydroxypyridinone and (ii) the TREN tertiary nitrogen (shown in Figure 2). This assertion is supported by the X-ray crystal structures of the Gd, La, and Fe complexes of **1**.[5,9,10] In order to probe the effect of this intramolecular hydrogen-bonding network on the stability of the Gd^{3+} complex, variations in the ligand scaffold were made. Insertion of a glycine (Gly) spacer between the TREN cap and the HOPO binding unit provides an expanded scaffold. Lengthening of the ethylene backbone of TREN to a propylene motif (TRPN) also increases the scaffold size. Therefore, while the scaffold size is varied, all three ligands remain tripodal and hexadentate and employ hydroxypyridinone units for metal binding. Herein, we describe the solution thermodynamics of [Gd(TREN-Gly-1-Me-3,2-HOPO)] (Gd-**2**) and [Gd(TRPN-1-Me-3,2-HOPO)] (Gd-**3**), highlighting the effect of scaffold size on complex stability. The water proton relaxivity properties of Gd-**2** are also reported.

Experimental Details

General Synthetic Considerations. Unless otherwise noted, all solvents and starting materials were obtained from commercial suppliers and used without further purification. Flash silica gel chromatography was performed using Merck silica gel (40−7 mesh). Microanalyses were performed by the Microanalytical Services Laboratory, and mass spectra were recorded at the Mass Spectrometry Laboratory, both of the College of Chemistry, University of California, Berkeley. Unless otherwise stated, NMR spectra were recorded at room temperature on either AMX-300, AM-400, AMX-400, or DRX-500 Brüker FT spectrometers.

Syntheses. Gly-1-Me-3,2-HOPO (6). The synthesis of 1-Me-3,2-HOPO-thiaz (**5**) is described elsewhere.[5] Compound **5** (3.00 g, 8.334 mmol) was dissolved in CH_2Cl_2 (50 mL) and 2-propanol (50 mL) and added to a solution of NaOH (0.350 g, 8.60 mmol) and glycine (0.626 g, 8.334 mmol) in water (3 mL). The yellow mixture was then stirred for 24 h. The solvent was evaporated and the product purified by flash column chromatography (SiO_2, CH_2Cl_2 with an increasing gradient of methanol from 0 to 10%). The solvent was evaporated and the product purified further by recrystallization from hot ethanol to afford white needles of **6** (yield: 2.06 g, 78%). ^{1}H NMR ($CDCl_3$, 300 MHz): $\delta = 3.61$ (s, 3H, N−CH_3), 4.05 (d, $J = 5.4$ Hz, 2H, glycine CH_2), 5.43 (s, 2H, Bn CH_2), 6.78 (d, $J = 7.2$ Hz, 1H, HOPO CH), 7.12 (d, $J = 7.2$ Hz, 1H, HOPO CH), 7.33−7.49 (m, 5H, ArH), 8.51 (t, $J = 5.4$ Hz, 1H, NH). ^{13}C NMR (d_6-DMSO, 125 MHz): $\delta = 37.08$, 41.30, 73.14, 103.08, 128.25, 128.93, 132.26, 133.99, 136.70, 144.58, 158.92, 163.80, 170.99. Anal. Calcd (Found) for $C_{16}H_{16}N_2O_5$: C, 60.75 (60.84); H, 5.10 (5.11); N, 8.86 (8.70). (+) EI-MS: m/z 317 $[MH]^+$.

TREN-Gly-1-Me-3,2-HOPO−Bn (7). *N*-Hydroxysuccinimide (0.534 g, 4.64 mmol) was added to a solution of **6** (1.220 g, 3.87 mmol) in dry THF (60 mL) under a N_2 atmosphere. After stirring for 20 min, dicyclohexylcarbodiimide (DCC, 0.956, 4.64 mmol) and (dimethylamino)pyridine (DMAP, 0.044 g, 0.46 mmol) were added. After 9 h, a white precipitate of dicyclohexylurea (DCU) had formed, and the formation of the NHS-activated ester was judged to be complete by TLC. Tris(2-aminoethyl)amine (TREN, 0.141 g, 0.967 mmol) was added. Then small portions of TREN were added to the solution with at least 8 h between subsequent additions until the reaction was judged complete by TLC. The solvent was evaporated and the residue taken up in a 1.0 M aqueous solution of HCl (50 mL). The suspension was filtered and the filtrate washed with CH_2Cl_2 (2 × 50 mL). The combined organic fractions were then back-washed with 1.0 M HCl (50 mL) solution. NaOH solution (10 M) was added dropwise to the combined aqueous fractions until the pH reached 11. The aqueous fractions were then washed with CH_2Cl_2 (10 × 50 mL) and ethyl acetate (3 × 50 mL). The organic extracts were combined, dried (Na_2SO_4), and evaporated to dryness. The product was purified by flash column chromatography (SiO_2, CH_2Cl_2 with increasing gradient of methanol from 0 to 10%). Evaporation of the solvent afforded a white foam

(8) Xu, J.; Durbin, P. W.; Kullgren, B.; Raymond, K. N. *J. Med. Chem.* **1995**, *38*, 2606−2614.
(9) Cohen, S. M.; Xu, J.; Radkov, E.; Raymond, K. N.; Botta, M.; Barge, A.; Aime, S. *Inorg. Chem.* **2000**, *39*, 5747−5756.
(10) Xu, J.; O'Sullivan, B.; Raymond, K. N. *Inorg. Chem.* **2002**, *41*, 6731−6742.

(yield: 0.753 g, 56%). ^{1}H NMR ($CDCl_3$, 400 MHz): δ = 2.51 (m, 6H, TREN NCH_2), 3.20 (m, 6H, TREN $NHCH_2$), 3.51 (s, 9H, $N-CH_3$), 3.85 (d, J = 5.4 Hz, 6H, glycine CH_2), 5.42 (s, 6H, Bn CH_2), 6.59 (d, J = 7.2 Hz, 3H, HOPO), 7.00 (d, J = 7.2 Hz, 3H, HOPO), 7.27−7.51 (m, 18H, ArH and glycine-TREN NH), 8.58 (t, J = 5.4 Hz, 3H, HOPO-glycine NH). ^{13}C NMR ($CDCl_3$, 125 MHz): δ = 37.35, 43.07, 49.89, 53.80, 74.07, 104.03, 128.23, 128.40, 128.99, 130.11, 132.22, 135.63, 145.89, 159.14, 163.64. Anal. Calcd (Found) for $C_{54}H_{60}N_{10}O_{12}\cdot 2H_2O$: C, 60.21 (59.96); H, 5.99 (5.96); N, 13.00 (12.93). (+) FAB-MS: m/z 1041.5 $[MH]^+$.

TREN-Gly-1-Me-3,2-HOPO (2). Compound **7** (0.650 g, 0.624 mmol) was dissolved in a mixture of methanol (325 mL) and ethanol (325 mL) and added to a slurry of 5% Pd on C (0.65 g) in ethanol (65 mL). The reaction was stirred under an atmosphere of hydrogen for 6 h. The solution was filtered and the solvent removed by evaporation to afford a white solid (yield: 0.296 g, 62%). This solid was found to be hygroscopic and was therefore stored in a vacuum desiccator. ^{1}H NMR (d_6-DMSO, 400 MHz): δ = 2.54 (br m, 12H, TREN CH_2), 3.46 (s, 9H, $N-CH_3$), 3.92 (br s, 6H, glycine CH_2), 6.52 (d, J = 7.3 Hz, 3H, HOPO), 7.17 (d, J = 7.3 Hz, 3H, HOPO), 7.95 (br s, 3H, glycine-TREN NH), 8.71 (br s, 3H, HOPO-glycine NH). ^{13}C NMR (D_2O, 125 MHz): δ = 34.78, 37.52, 42.68, 54.49, 104.20, 116.79, 128.06, 146.50, 158.28, 166.15, 172.30. Anal. Calcd (Found) for $C_{33}H_{42}N_{10}O_{12}\cdot 3.5H_2O$: C, 47.54 (47.49); H, 5.92 (5.46); N, 16.80 (16.48). (+) FAB-MS: m/z 771 $[MH]^+$.

Gd(TREN-Gly-1-Me-3,2-HOPO) (Gd-2). $GdCl_3\cdot 6H_2O$ (0.0327 g, 0.124 mmol) was dissolved in a solution of **2** (0.100 g, 0.138 mmol) in H_2O (30 mL). Then, an excess of aqueous ammonia solution was added to yield a light yellow precipitate. The suspension was heated to 100 °C for 2 h. After cooling, the solution was reduced in volume and the product filtered and dried under vacuum (yield: 0.079 g, 71%). Anal. Calcd (Found) for Gd(TREN-Gly-1-Me-3,2-HOPO)$(H_2O)_2\cdot 3H_2O$, $C_{33}H_{43}N_{10}O_{14}Gd\cdot 3H_2O$: C, 39.05 (39.37); H, 4.87 (4.42); N, 13.80 (13.37); Gd, 15.49 (15.35). (+) FAB-MS: m/z 924 $[MH]^+$.

Solution Thermodynamics. Equilibrium constants were measured at 25 °C in aqueous solution with a supporting electrolyte of 0.1 M KCl. They were determined as cumulative formation constants (β_{mlh}, where M, L, and H refer to the metal, ligand, and proton species, respectively). For convenience, the protonation reactions of the Gd complexes are occasionally discussed as stepwise protonation constants (K_{11h}).

$$m\mathrm{M} + l\mathrm{L} + h\mathrm{H} \leftrightarrow \mathrm{M}_m\mathrm{L}_l\mathrm{H}_h$$

$$\beta_{mlh} = \frac{[\mathrm{M}_m\mathrm{L}_l\mathrm{H}_h]}{[\mathrm{M}]^m[\mathrm{L}]^l[\mathrm{H}]^h} \qquad K_{11h} = \frac{[\mathrm{MLH}_h]}{[\mathrm{MLH}_{h-1}][\mathrm{H}]} = \frac{\beta_{11h}}{\beta_{11(h-1)}}$$

The titration apparatus has been previously described.[6,10,11] Electrode calibration was performed by strong acid/strong base titration,[6] with analysis of calibration data using the program GLEE.[12] For measurements to low pH (<2.5), a correction was applied for the variation in electrode junction potentials.[6]

Ligand Protonation Constants. Ligand protonation constants were determined for **2**. These experiments were performed by dissolving a weighed portion of the ligand in electrolyte solution (giving ~7×10^{-4} M) with an addition of acid to protonate the fourth basic site. The material was titrated to high pH with KOH and in reverse with HCl. Three experiments were performed yielding six titrations in all.

Table 1. Determined Protonation and Formation Constants and Calculated pM Values for the Indicated Gd/Ligand Systems[a]

scaffold	**2**		**1**[10,11]		**3**[10]	
mlh	log β_{mlh}	log K_{11h}	log β_{mlh}	log K_{11h}	log β_{mlh}	log K_{11h}
011	6.96(4)		8.19		9.43	
012	13.34(1)		15.16		16.14	
013	19.30(3)		20.99		22.16	
014	24.52(1)		25.96		27.53	
110	15.92(6)		19.22		16.5(2)	
111	21.9(1)	6.0	22.75	3.53	23.9(1)	7.4
112	24.90(2)	3.1	26.23	3.48	26.6(1)	2.7
pM	16.7		19.2		15.6	

[a] All values are the result of at least three independent measurements. Figures in parentheses give the standard deviation in the least significant figure as determined by the variation between determinations. Values given without a standard deviation are taken from previously published reports.[10,11] pM values give the free metal concentration calculated using the formation constants in the table and the conditions of pH 7.4, [Gd] = 1×10^{-6}, and [L] = 1×10^{-5} M.

The pairwise sets of protonation titrations were combined for simultaneous refinement using the program HYPERQUAD.[13] Both proton and ligand concentrations were refined with the shifts in ligand concentration for each pair of titrations being constrained to be equal. All data sets were truncated to pH 8 and below; some irreversibility was noted in experiments taken above this level. The resulting protonation constants are given in Table 1.

Gd Complexation Constants. Gd complexation constants were determined for ligands **2** and **3**. Two distinct strategies were used. In the "mid-pH range" experiments, equimolar solutions of the metal and respective ligand (10% excess of ligand) were titrated over the pH range 3−7 with spectral and potentiometric measurements being recorded. Collection of spectrophotometric measurements required a relatively dilute (~50 μM) concentration of the complex so an external source of pH buffering was added to the solutions (MES buffer, ~5×10^{-4} M). Each pair of titrations (i.e., forward against KOH and reverse against HCl) was combined for simultaneous refinement. Low pH range (1.5−3.5) experiments were performed with similar concentrations of the complex. These titrations were only performed to low pH and not back to pH 3.5. Addition of an extra buffer in this latter case was unnecessary since water itself has sufficient buffering capacity to allow accurate pH measurement at such extreme values.

Spectral data derived from the titrations with Gd^{3+} were analyzed using again the program Hyperquad, and the closely related program pHAB.[14] Typically a spectrum comprising ~60 absorbance measurements at wavelengths between 250 and 380 nm and a pH measurement were included in the refinement for each point in the titrations. Nonlinear least-squares analysis gave global σ values having an average value of 3.3 (range 2.6−4.6 over all titrations). The resulting complex formation constants are given in Table 1

Relaxometric Studies. Water proton $1/T_1$ longitudinal relaxation rates (20 MHz, 25 °C) were measured with a Stelar Spinmaster Spectrometer (Mede, Pv, Italy) on 0.1−0.3 mM aqueous solutions of the complexes at pH = 7.1, I = 0.1. ^{1}H spin−lattice relaxation times T_1 were acquired by the standard inversion−recovery method with a typical 90° pulse width of 3.5 ms, 16 experiments of 4 scans. The reproducibility of the T_1 data was ±1%. The temperature was controlled with a Stelar VTC-91 air-flow heater equipped with a copper−constantan thermocouple (uncertainty of ±0.1 °C).

(11) Doble, D. M. J.; Melchior, M.; O'Sullivan, B.; Siering, C.; Xu, J.; Raymond, K. N. *Inorg. Chem*., submitted.
(12) Gans, P.; O'Sullivan, B. *Talanta* **2000**, *51*, 33−37.
(13) Gans, P.; Sabatini, A.; Vacca, A. *Talanta* **1996**, *43*, 1739−1753.
(14) Gans, P.; Sabatini, A.; Vacca, A. *Ann. Chim. (Rome)* **1999**, *89*, 45−49.

Scheme 1. Synthesis of **2** and Gd-**2**[a]

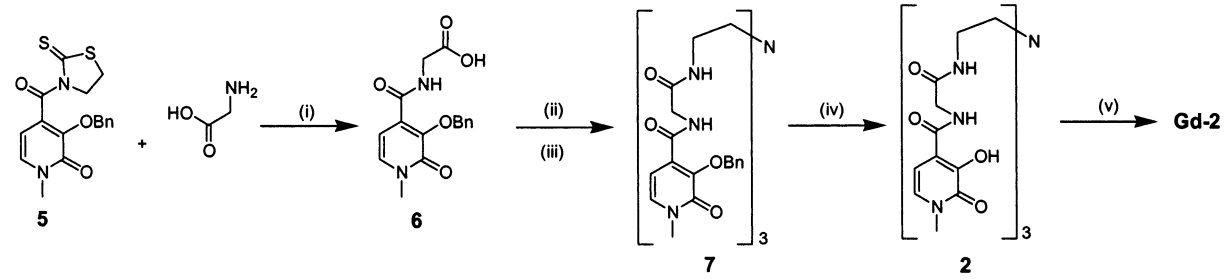

[a] (i) NaOH; (ii) NHS, DCC; (iii) TREN; (iv) 5% Pd/C, H_2; (v) $GdCl_3$, $NH_{3(aq)}$.

The $1/T_1$ nuclear magnetic relaxation dispersion (NMRD) profiles of water protons were measured over a continuum of magnetic field strength from 0.00024 to 0.28 T (corresponding to 0.01−12 MHz proton Larmor frequency) on the fast field-cycling Stelar Spinmaster FFC relaxometer installed at the "Laboratorio Integrato di Metodologie Avanzate", Bioindustry Park del Canavese (Colleretto Giacosa, To, Italy). The relaxometer operates under complete computer control with an absolute uncertainty in the $1/T_1$ values of ±1%. Additional data points at 20 and 90 MHz were recorded on a Stelar Spinmaster and on a JEOL Ex-90 spectrometers, respectively. A 0.3 mM aqueous solution of the complex at pH 7.3 was utilized for the measurements.

Results and Discussion

Synthesis. The design of ligand **2** follows suggestions by Shanzer and co-workers[15] that metal complex stability in similar tripodal catechol-amide type ligands may be enhanced by interstrand hydrogen bonding from the amide protons to phenolic oxygens. Studies on analogues of the siderophores corynebactin and enterobactin also indicate that the addition of the glycine spacer enhances the stability of the ferric complex.[16] The glycine derivative of **1** was synthesized as illustrated in Scheme 1. Coupling of thiazolide-activated **5** with glycine produces the Gly-HOPO intermediate (**6**) in reasonable yields. Activation of **6** with *N*-hydroxysuccinimide followed by coupling with TREN produces the Bn-protected TREN-Gly-1-Me-3,2-HOPO ligand (**7**). Deprotection by hydrogenation gave the final ligand (**2**) followed by complexation with $GdCl_3$ to provide Gd-**2**. TRPN-1-Me-3,2-HOPO (**3**) was synthesized as previously reported.[10]

Solution Thermodynamics. The ligand series presented in this work were examined by thermodynamic evaluation of their protonation and Gd^{3+} complex formation constants (Table 1). Such studies have been previously reported for the parent ligand **1**[5,11] and homotripodal structural analogues.[6,17] The glycine-spaced ligand, **2**, was observed to be distinctly more acidic than its parent, as shown by the value of β_{014} in Table 1 (24.52, compared with 25.96 and 27.53 for **1** and **3**, respectively).[10,11] It is quite possible that the extra amide groups present in the glycine-spaced ligand are better able to hydrogen bond with the acidic functional groups (Figure 2), thus stabilizing their deprotonated forms and lowering the acidity constants. A similar process may give rise to the opposite effect in **3**, the most basic ligand of the series. Here the expansion to propylene-bridged arms in the scaffold sets the tertiary amine more remote from the amide protons with the result that it displays a relatively basic protonation constant (log β_{011} = 9.43). These interactions in ligands **1** and **3** have been recently discussed elsewhere.[10] The spectral changes observed upon coordination by Gd^{3+} closely resemble those seen for other tripodal 3,2-HOPO-based ligands[6,9,11,17] and are illustrated in Figure 3.

The chemical model employed in the fitting of the Gd^{3+} titration data closely resembles that applied in related ligand systems,[6,9,11,17] with the formation of a monomeric complex with stepwise addition of up to two protons before the complex dissociates in strongly acidic media (below pH 2). Formation of the twice protonated species, $[GdLH_2]^{2+}$, which has been observed for all coordination systems containing gadolinium and tripodal HOPO-based ligands that have been studied to date,[6,9,11,17] is notable in the present case of the

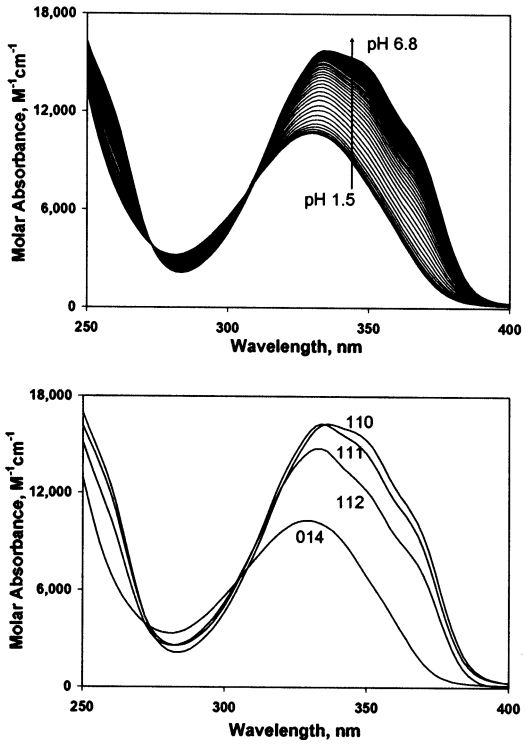

Figure 3. Molar absorptivity in the Gd^{3+}/**2** system. The lower diagram gives the spectra for the individual species as determined in the course of nonlinear least squares refinement of formation constants with the labels indicating the *mlh* stoichiometric coefficients, i.e., 112 = $[GdLH_2]^{2+}$.

(15) Tor, Y.; Libman, J.; Shanzer, A.; Felder, C. E.; Lifson, S. *J. Am. Chem. Soc.* **1992**, *114*, 6661−6671.
(16) Dertz, E.; Raymond, K. N. In *Abstracts of the 35th International Conference on Coordination Chemistry*; Heidelberg, Germany, 2002.
(17) Hajela, S.; Johnson, A. R.; Xu, J.; Sunderland, C. J.; Cohen, S. M.; Caulder, D. L.; Raymond, K. N. *Inorg. Chem.* **2001**, *40*, 3208−3216.

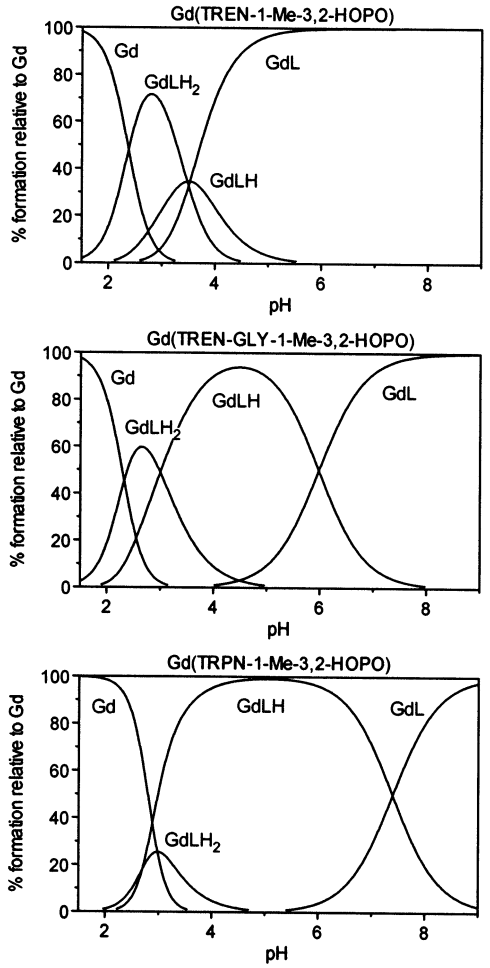

Figure 4. Species distribution diagrams calculated for 1 μM Gd^{3+} and 10 μM ligand.

glycine-spaced ligand, **2**, since this architecture creates a highly flexible scaffold. Therefore, it seems unlikely that the doubly protonated species arises from constraints imposed by the ligand scaffold. Rather, it represents an important geometry for this class of complexes. As discussed later, the origin of this doubly protonated species is assigned to protonation of both the capping amine and of one of the hydroxypyridinone arms. Coordination of the protonated HOPO moiety to the metal center remains possible when the phenolate oxygen together with its adjacent amide oxygen combine to give a salicylate mode of binding.[18] Assignment of the other proton added to such complexes to protonation at the capping amine has been established in a closely related study.[10]

Relative comparison of the coordination systems is provided in the species distribution diagrams of Figure 4. In all cases, coordination of the metal center begins with formation of the $[GdLH_2]^{2+}$ species. This species reaches a maximum at pH $\sim$ 2.5 and soon becomes deprotonated to form $[GdLH]^{+}$. This is reflected in all systems having a roughly equal value of $\sim$3.1 for log K_{112} (= 3.48, 3.1, and 2.7 for **1**, **2**, and **3**, respectively). The concurrence of these values over the current series of ligands is consistent with this protonation step occurring remote from the capping scaffold, i.e., protonation of one of the HOPO units, as already suggested. In contrast, the three complexes show large variation in the value of K_{111}, corresponding to the final deprotonation step to form $[GdL]^{0}$. A value of log K_{111} = 3.53 is observed for Gd-**1** while the Gd-**2** complex does not become deprotonated until higher pH, displaying a log K_{111} value of 6.0. The complex formed with **3** does not attain its final deprotonated form until pH values higher than its log K_{111} value of 7.4. This trend in values is consistent with the underlying reaction being assigned to protonation of the ligand scaffold and is fully consistent with a recent study of the ferric complexes of **1** and **3**.[10]

In Gd-**1**, the amine is the most acidic (log K_{111} = 3.53) because its central amine is held in the closest proximity to the amide protons due to the smaller size of the scaffold and greater rigidity present in the metal complex (Figure 2). Conversely for Gd-**3**, the value of log K_{111} is weakly basic, 7.4, consistent with the decreased ability of the central amine to hydrogen bond with the amide protons due to cap enlargement (Figure 2). This value is virtually identical to the equivalent value observed for the iron complex of the same ligand, i.e., log K_{111} = 7.72.[10] The log K_{111} value for Gd-**2** is 6.0, identical with the acidity previously reported for the tris(acetyl) derivative of TREN (Ac_3TREN).[10,19] The tertiary amine within the scaffold of Gd-**2** exists in an environment closely resembling that of Ac_3TREN, in which the three amide groups increase the acidity of the central amine via hydrogen-bonding effects. The possible H-bonding motifs resulting from the protonation of the tertiary amine for Gd-**1**, Gd-**2**, and Ac_3TREN are illustrated in Scheme 2. Protonation of Ac_3TREN is expected to result in the formation of an H-bond between an amide oxygen and the proton of the tertiary amine. The similarity in the values of log K_{011} of Ac_3TREN and of log K_{111} for Gd-**2** supports the notion of a similar H-bonding process in the complex (as illustrated in Scheme 2). Thus, a structure in which the amide protons of the glycine spacers lie within the central cavity of complex Gd-**2**, as illustrated at the extreme right-hand side of Scheme 2, is considered unlikely since these amide protons would lead to increased acidity of the central amine. In such a case, a value of log K_{111} closer to that observed for Gd-**1**, i.e., between 3 and 4, would be expected.

The pM values of the ligands (Table 1) indicate the following trend in gadolinium complex stability: Gd-**1** (19.2) > Gd-**2** (16.7) > Gd-**3** (15.6). Clearly, expansion of the ligand scaffold has had a detrimental effect in both cases. This indicates a failure of the original design motif for **2**, i.e., that the insertion of glycine spacers may lead to a complex stability enhancement via interstrand hydrogen bonding. Support for this conclusion is also provided by a recently determined X-ray crystal structure of the ferric complex of **2**, which indicates the absence of interstrand hydrogen bonding,[20] contrary to reports of Shanzer and co-workers for TREN catecholamides with amino acid spacers.[15]

(18) Cohen, S. M.; O'Sullivan, B.; Raymond, K. N. *Inorg. Chem.* **2000**, *39*, 4339−4346.

(19) Cohen, S. M.; Meyer, M.; Raymond, K. N. *J. Am. Chem. Soc.* **1998**, *120*, 6277−6286.

(20) Xu, J.; Raymond, K. N. Unpublished results.

Scheme 2. Proposed Intramolecular Hydrogen Bonding Motifs in Gd-**1**, Ac_3TREN, and Gd-**2**

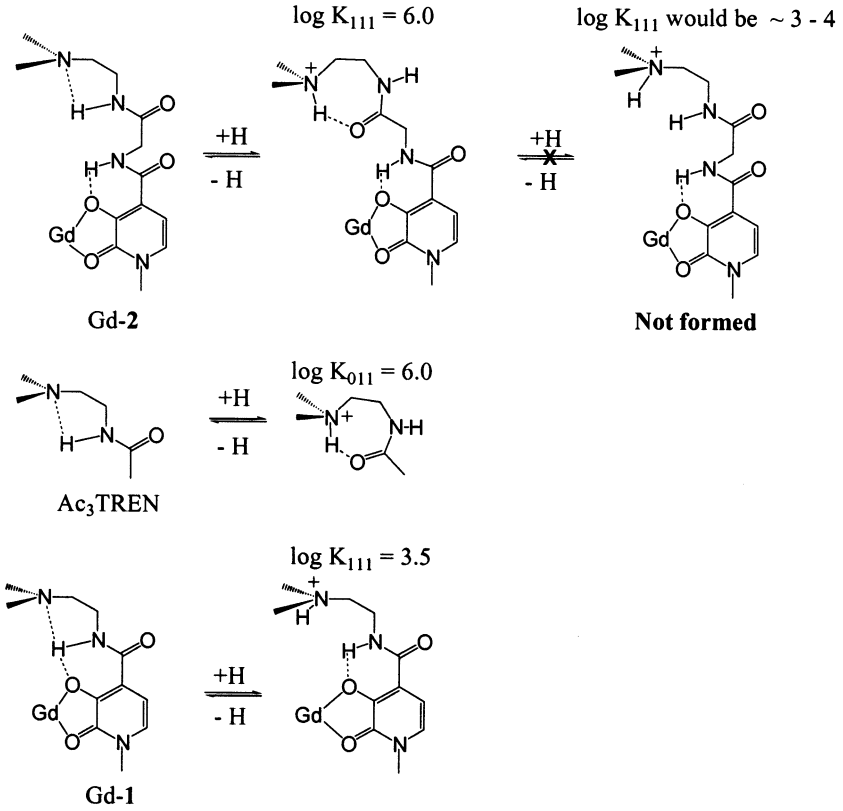

Relaxometric Studies. The relaxametric properties of Gd-**2** were investigated and compared with those of Gd(L-Ser-TREN-1-Me-3,2-HOPO) (Gd-**4**), a structural analogue of the parent complex (Gd-**1**). The relaxivity of Gd-**2** is 6.6 mM^{-1} s^{-1} (20 MHz, 25 °C, pH 7.3), a value lower than that found for Gd-**1** and Gd-**4**[7] (r_{1p} = 9.0 mM^{-1} s^{-1}), but still greater than that of Gd(DTPA) ($r_{1p} \sim 4.5$ mM^{-1} s^{-1}).[1] Unlike Gd-**4** and the other related complexes, Gd-**2** does not show a change of relaxivity with pH in the range 1−8 (Figure 5). Only at pH values greater than pH 8 is there a decrease in $r_{1p,}$ which is often observed in systems with $q > 1$ and explained by the displacement of the water molecules by carbonate anions (dissolved CO_2) or formation of hydroxo species.[21] In the present case, partial precipitation of the complex at basic pH where the unprotonated, neutral species predominates in solution (Figure 4) cannot be excluded. We have assumed that the relaxivity peak around pH = 2−3 often observed previously for this family of complexes is related to an increase of the hydration number (q) from 2 to 3 and the coordination of the Gd^{3+} passes from 8 to 9. As the ligand is more flexible, the changes in the geometry of the cap following protonation are less likely to produce large effects on the coordination cage. An alternative explanation to the relaxivity peak at low pH could be the occurrence of prototropic exchange.[22] The effect of the exchange of this proton on the relaxivity would be much attenuated with the introduction of a spacer (complex **2**). However, this possibility has to be ruled out since the increase in relaxivity observed from pH 7 to 2 is about 5 mM^{-1} s^{-1}, too large for the contribution of a single proton at a relatively long distance from the paramagnetic center.

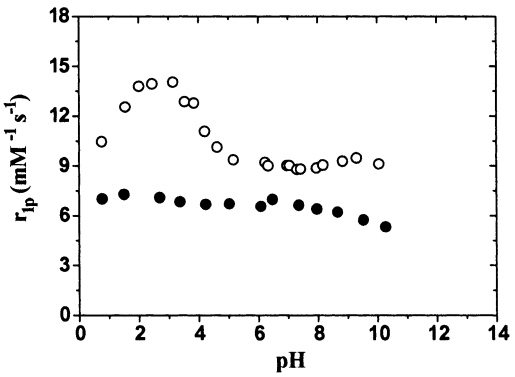

Figure 5. Plot of ^1H relaxivity, r_{1p}, versus pH at 20 MHz and 25 °C for Gd-**2** (●) and Gd-**4** (○).

The nuclear magnetic relaxation dispersion (NMRD) profile of Gd-**2** was measured both at pH 4.0 and pH 7.3 at 25 °C. The two profiles are identical to support the described hypothesis that the complex maintains the same coordination geometry between pH 8 and 2. For comparison, the profile of Gd-**4** is also shown (Figure 6), and it is observed that the relaxivity of the two complexes differs primarily in the high magnetic field strength region, corresponding at proton Larmor frequencies above ca. 5 MHz. The experimental data were analyzed in terms of the Solomon−Bloembergen−Morgan (SBM)[23,24] and Freed[25] equations for inner-sphere

(21) Aime, S.; Botta, M.; Geninatti Crich, S.; Giovenzana, G.; Pagliarin, R.; Sisti, M.; Terreno, E. *Magn. Reson. Chem.* **1998**, *36*, S200−S208.
(22) Aime, S.; Botta, M.; M., F.; Terreno, E. *Acc. Chem. Res.* **1999**, *32*, 941−949.
(23) Bloembergen, N.; Morgan, L. O. *J. Chem. Phys.* **1961**, *34*, 842−850.
(24) Banci, L.; Bertini, I.; Luchinat, C. *Nuclear and Electronic Relaxation*; VCH: Weinheim, 1991.

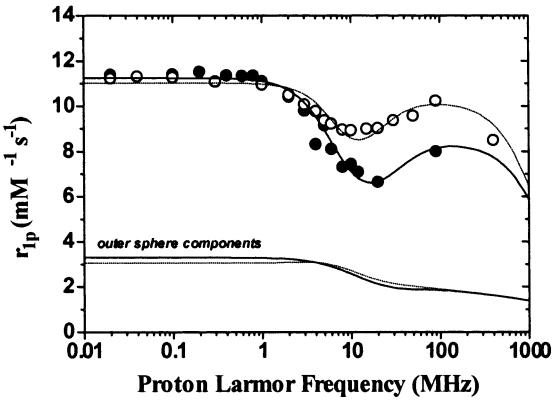

Figure 6. NMRD profiles for Gd-**2** (●) and Gd-**4** (○) at 25 °C and pH = 7.0. The curves through the data points are calculated with the best fitting parameters of Table 2. The lower curves show the outer-sphere component of the relaxivity for Gd-**2** (—) and Gd-**4** (···).

Table 2. Best Fitting Parameters Determined by Analysis of NMRD Profiles for Gd-**2** and Gd-**4** at 25 °C and pH 7.0

	Gd-**4**	Gd-**2**
Δ^2 ($s^{-2} \times 10^{19}$)	8.3	13.5
τ_V (ps)	20	10
τ_R (ps)	129	110
r (Å)	3.08	3.12
q	2	2

and outer-sphere contributions, respectively. The inner-sphere term depends on q, their mean residence lifetime (τ_M), the water proton−gadolinium distance (r), τ_R, the electronic relaxation time at zero-field (τ_{S0}), and the correlation time for the modulation of τ_{S0} (τ_V). The outer-sphere contribution depends on τ_{S0}, τ_V, the distance of closest approach between the paramagnetic center and the diffusing water protons (d), and their relative diffusion constant (D). A hydration number (q) of 2 was assumed (on the basis of the X-ray crystal structure of Gd-**1**)[5] as well as standard values for a (3.8 Å) and D (2.24×10^{-5} cm^2 s^{-1}).

The fitting of the curves (Table 2) indicates that this large difference is mostly due to a relatively small difference in the parameters of the electron spin relaxation: Δ^2 and τ_V (Δ^2 = mean-square zero-field-splitting energy = $1/[12\tau_V\tau_{SO}]$). This is also clearly shown by the calculated profiles of the outer-sphere component (lower curves in Figure 6) which differ only in the low field region. A larger value of Δ^2 often has been found associated with Gd^{3+} complexes of low symmetry[1,26] and high flexibility: the axially symmetric and stereochemically rigid macrocyclic complex Gd(DOTA) has a Δ^2 value of 1.3×10^{19} s^{-1}, whereas the highly fluxional Gd(DTPA) presents a Δ^2 value of 4.2×10^{19} s^{-1}.[1,3] This only represents an empirical rule as the chemical nature of the coordinating groups may also play a significant role (e.g., DOTA vs DOTP),[22,27] but in general, this parameter is smaller for complexes of macrocyclic ligands than in the case of the complexes with the corresponding acyclic ligands.[3] The present data confirm this trend as the more flexible Gd-**2** has a Δ^2 value almost twice that of Gd-**4**.

The complex Gd-**2** has a water solubility of 0.37 mM (25 °C, 0.1 M NaCl) which precluded studies on the water exchange rate by ^{17}O NMR. Thus, in the fitting of the NMRD profile, the value τ_M was set to 10 ns (similar to the value of 14 ns found for Gd-**4**).[7] However, changing the τ_M value from 5 to 50 ns affects the fitting result less than 1%, as expected for a low molecular weight complex for which the rotational correlation time (τ_R) represents the dominant contribution to the overall correlation time (τ_C) characterizing the modulation of the dipolar interaction.[3,22] The NMRD and pH-relaxivity profiles of Gd-**1** and Gd-**3** were not determined due to the low solubility of the complexes (<0.1 mM).

Conclusions

Solution thermodynamics analysis of complex stability in structural analogues of the parent complex (Gd-**1**) has been presented. Introduction of glycine spacers results in a more acidic ligand (**2**) with lower affinity for Gd^{3+} than the parent ligand (**1**). The pH-independent relaxivity of Gd-**2** indicates a constant hydration number of 2 across a wide pH range. A lengthening of the TREN cap enhances the basicity of **3** but also results in a loss of complex stability (Gd-**3**). These effects are consistent with the effects of proposed hydrogen bonding between the amide protons and both the scaffold amine and the HOPO phenol groups. Ligand **3** displays the least affinity for Gd^{3+} at pH 7.4, as reflected in the pM values. Nevertheless, the stability of Gd-**3** remains at least equal to that of Gd(DTPA-BMA), a MRI contrast agent in clinical use (Omniscan). The decrease in the Gd complex stability at pH 7.4 with an increase in ligand basicity is in agreement with a recently reported study.[11] While extension of the ethylene spacers within the ligand cap to propylene units apparently leads to disruption of intramolecular H-bonding, and ligand basicity is an important factor in determining Gd^{3+} complex stability,[11] these results demonstrate that ligand structural factors, such as scaffold size, also play an important role in determining the Gd^{3+} complex stability. This is important for the development of these complexes as potential high-relaxivity, nontoxic contrast agents for MRI.

Acknowledgment. Support from the NIH (Grant HL69832) and a research gift from Schering A.G. are gratefully acknowledged. S.A. and M.B. acknowledge support from MIUR and CNR.

IC0261575

(25) Hwang, L. P.; Freed, J. H. *J. Chem. Phys.* **1975**, *63*, 4017−4025.
(26) Aime, S.; Botta, M.; Ermondi, G.; Fedeli, F.; Uggeri, F. *Inorg. Chem.* **1992**, *31*, 1100−1103.
(27) Aime, S.; Botta, M.; Terreno, E.; Anelli, P. L.; Uggeri, F. *Magn. Reson. Med.* **1993**, *30*, 583−591.